Coherently induced grating in refractive index enhanced medium*

Zhuan-Zhuan Liu(刘撰撰), Yu-Yuan Chen(陈煜远), Jia-Yu Yuan(原佳宇), and Ren-Gang Wan(万仁刚)†

School of Physics and Information Technology, Shaanxi Normal University, Xi'an 710062, *China*

(Received 5 April 2017; revised manuscript received 15 July 2017; published online 20 October 2017)

We demonstrate a scheme for coherently induced grating based on a mixture of two three-level atomic species interacting with two standing-wave fields. As a result of interaction between the absorptive and amplified Raman resonances, the refractive index of the medium can be enhanced and modulated periodically. Then a sinusoidal grating, which can diffract the probe field into high-order directions, is coherently formed in the medium. The proposed scheme is theoretically investigated in a mixture of atomic isotopes of rubidium. The results show that the diffraction efficiency depends strongly on the two two-photon detunings of the two Raman transitions and the intensities of the two driving standing-wave fields. The proposed electromagnetically induced grating scheme may be applied to the all-optical switching and beam splitting in optical networking and communication.

Keywords: refractive index enhancement, electromagnetically induced grating, electromagnetically induced transparency, active Raman gain

PACS: 42.50.Gy, 42.65.An, 42.25.Fx **DOI:** 10.1088/1674-1056/26/12/124209

1. Introduction

Recently, the research of light-media interaction has played a significant role in the area of quantum optics, where many interesting optical phenomena can be caused by atomic coherence and quantum interference. Of them, the electromagnetically induced transparency (EIT) is the most typical.[1,2] The EIT is mainly used to manipulate the refractive and dispersive properties by suppressing or eliminating the absorption for a weak probe beam in atomic medium driven by an additional strong coherent field. Meanwhile, coherent population trapping (CPT) state,[3,4] or the so-called dark state, can be formed in this process. The principal mechanisms for EIT and CPT have been explored in many recent applications, such as lasing without inversion,[5,6] refractive index enhancement,[7,8] slow light,[9,10] light storage,[11,12] enhanced Kerr nonlinearity,[13,14] optical solitons,[15,16] etc.

As is well known, an electromagnetically induced grating (EIG) can be created in a medium by replacing the travelling-wave driving field in EIT with a standing-wave. The probe field will obtain a periodic variation of absorptive coefficient due to the spatial modulation induced by the standing-wave field. At the same time, the refractive index also changes periodically.[17] Then the medium is equivalent to a grating on which the resonant probe beam can be diffracted into high-order directions. This phenomenon has been observed experimentally in cold and hot atomic samples[18,19] and universally applied to optical bistability,[20] all optical switching and routing,[21] beam splitting and fanning,[22] quantum Talbot effect,[23,24] surface solitons,[25] photonic Floquet topological insulators,[26] etc. However, the diffraction efficiency of EIG is not enough due to the inevitable atomic absorption. Therefore, an electromagnetically induced phase grating (EIPG) was proposed for high diffraction efficiency by using enhanced Kerr nonlinear refractivity at low light level.[27,28] Likewise, one can build gratings in other media or configurations such as quantum well,[29] quantum dot,[30] molecular magnets,[31] double-dark resonances system,[32,33] phase-dependent system[34] and CPT system.[35] Meanwhile, a kind of gain-phase or gain grating based on the effect of active Raman gain (ARG) has been put forward to obtain much higher diffraction efficiency in high-order directions.[36] Recently, Wang *et al.* extended EIG to the two-dimensional (2D) case and achieved an electromagnetically induced cross-grating (EICG) in a four-level tripod-type atomic system.[37] Then, schemes for EICG based on EIT or ARG in multi-level atomic systems were proposed, and the diffraction efficiencies were improved.[38–41]

In this paper, we theoretically investigate a one-dimensional (1D) phase grating coherently induced in a mixture of two species of Λ-type atomic system with EIT and ARG, respectively. This three-level atomic system has been proposed for the enhancement of refractivity without absorption.[42,43] Recently, the creation of a spatially distributed PT-symmetric refractive index was explored.[44] Here, by using two far-detuned standing-wave fields to drive the corresponding atomic transitions in the vicinity of two-photon resonance, we obtain spatial absorption-phase, pure-phase, and gain-phase gratings through modulating the interaction of the two Λ schemes. Thus, the probe beam can be diffracted to high-order directions with different intensities. It is found that the diffrac-

*Project supported by the National Natural Science Foundation of China (Grant Nos. 11204367 and 61475191) and the Fundamental Research Funds for the Central Universities, China (Grant Nos. GK201503022 and GK201601008).

†Corresponding author. E-mail: wrg@snnu.edu.cn

© 2017 Chinese Physical Society and IOP Publishing Ltd

tion efficiency of the grating depends on the detunings of the two two-photon Raman transitions and the amplitudes of the standing-wave fields. We also analyze the physical mechanism for such a mixture of EIT and ARG in a real atomic system with ^{85}Rb and ^{87}Rb. The scheme can be used as all-optical switching and beam splitter which have potential applications in optical networking and communication.

2. Model and equations

The considered atomic system is a mixture of two three-level Λ-type atomic species (EIT and ARG) interacting with three coherent laser fields as illustrated in Fig. 1. The atomic densities of the species are N_1 and N_2, respectively. Then the total atomic density is $N = N_1 + N_2$. Each of Λ systems is marked by si $(i = 1,2)$ with one excited state $|3,si\rangle$ and two ground levels $|1,si\rangle$ and $|2,si\rangle$. A weak probe field with frequency ω_p and a pair of coupling fields with frequencies ω_{s1} and ω_{s2} drive the corresponding transitions. The Rabi frequencies of the driving fields are denoted as $\Omega_{si} = \mu_{lm,si}E_{si}/2\hbar$ and $\Omega_{pi} = \mu_{lm,si}E_p/2\hbar$ $(i = 1,2)$, where E_{si} and E_p represent the amplitudes of electric fields and $\mu_{lm,si}$ $(l,m = 1, 2, 3)$ are the dipole moments of the corresponding transitions. We define that $\Delta_{s1} = \omega_{31,s1} - \omega_{s1}$ and $\Delta_{s2} = \omega_{32,s2} - \omega_{s2}$ are the one-photon detunings for the two coupling fields, and $\Delta_{p1} = \omega_{32,s1} - \omega_p$ and $\Delta_{p2} = \omega_{31,s2} - \omega_p$ are the detunings for the probe field with $\omega_{lm,si}$ $(l,m = 1,2,3; i = 1,2)$ being the resonant frequencies of corresponding transition in si-system. Here, all the involved fields are detuned far from the excited state $|3,si\rangle$. For the EIT system, the atom is transparent to the probe field under the condition of two-photon resonance, i.e., $\delta_1 = 0$, and its refractive index is unity. However, one can obtain a narrow absorption peak near the two-photon resonance.[45] At the same time, the refractivity is enhanced due to the Raman process. For the ARG system, the probe field can be amplified by the atoms and a nonzero susceptibility is then achieved when the two-photon detuning $\delta_2 \neq 0$. The combination of Raman absorption and Raman gain can result in enhanced refractivity with vanishing absorption. The laser driven ^{85}Rb and ^{87}Rb atoms can be utilized as the two three-level Λ systems, of which one provides an absorption resonance and the other induces a gain resonance for the probe beam.[42,43]

In the framework of the semiclassical theory, with the rotating-wave approximation and the electric-dipole approximation, the Hamiltonian of si-system in the interaction picture can be written as

$$\begin{aligned} H_{s1} &= \hbar\delta_1 |2,s1\rangle\langle 2,s1| + \hbar(\Delta_{s1}+\delta_1)|3,s1\rangle\langle 3,s1| \\ &\quad -\hbar[\Omega_{s1}|1,s1\rangle\langle 3,s1| + \Omega_{p1}|2,s1\rangle\langle 3,s1| + \text{H.C.}], \quad (1a) \\ H_{s2} &= \hbar\delta_2 |2,s2\rangle\langle 2,s2| + \hbar(\Delta_{s2}+\delta_2)|3,s2\rangle\langle 3,s2| \\ &\quad -\hbar[\Omega_{p2}|1,s2\rangle\langle 3,s2| + \Omega_{s1}|2,s2\rangle\langle 3,s2| + \text{H.C.}]. \quad (1b) \end{aligned}$$

In Eq. (1), the quantities δ_1 and δ_2 are the two-photon detunings of the laser beams from each Raman transition, and they are defined as $\delta_1 = \omega_{s1} - \omega_{21,s1} - \omega_p$ and $\delta_2 = \omega_{s2} + \omega_{21,s2} - \omega_p$, respectively.

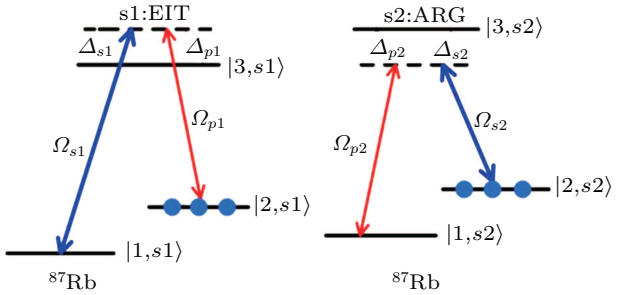


Fig. 1. (color online) Energy level scheme based on a mixture of two species of Λ atomic system driven by three light fields. The initially populated levels are indicated by the dots.

By using the Liouville equation, we obtain the relevant density-matrix equations as follows:

$$\begin{aligned} \mathrm{i}\dot{\rho}_{21,s1} &= \delta_1\rho_{21,s1} - \Omega_{p1}\rho_{31,s1} + \Omega_{s1}\rho_{23,s1} - \mathrm{i}\gamma_{21,s1}\rho_{21,s1}, \quad (2a) \\ \mathrm{i}\dot{\rho}_{31,s1} &= -\Omega_{s1}(\rho_{11,s1} - \rho_{33,s1}) - \Omega_{p1}\rho_{21,s1} \\ &\quad + (\Delta_{s1}+\delta_1)\rho_{31,s1} - \mathrm{i}\gamma_{31,s1}\rho_{31,s1}, \quad (2b) \\ \mathrm{i}\dot{\rho}_{32,s1} &= -\Omega_{s1}\rho_{12,s1} - \Omega_{p1}(\rho_{22,s1} - \rho_{33,s1}) \\ &\quad + \Delta_{s1}\rho_{32,s1} - \mathrm{i}\gamma_{32,s1}\rho_{32,s1}, \quad (2c) \\ \mathrm{i}\dot{\rho}_{21,s2} &= \delta_2\rho_{21,s2} - \Omega_{s2}\rho_{31,s2} \\ &\quad + \Omega_{p2}\rho_{23,s2} - \mathrm{i}\gamma_{21,s2}\rho_{21,s2}, \quad (2d) \\ \mathrm{i}\dot{\rho}_{31,s2} &= -\Omega_{p2}(\rho_{11,s2} - \rho_{33,s2}) - \Omega_{s2}\rho_{21,s2} \\ &\quad + (\Delta_{s2}+\delta_2)\rho_{31,s2} - \mathrm{i}\gamma_{31,s2}\rho_{31,s2}, \quad (2e) \\ \mathrm{i}\dot{\rho}_{32,s2} &= -\Omega_{p2}\rho_{12,s2} - \Omega_{s2}(\rho_{22,s2} - \rho_{33,s2}) \\ &\quad + \Delta_{s2}\rho_{32,s2} - \mathrm{i}\gamma_{32,s2}\rho_{32,s2}, \quad (2f) \end{aligned}$$

with $\sum_{l=1}^{3}\rho_{ll,si} = 1$ and $\rho_{lm,si} = \rho^*_{ml,si}$. In the above equations, we consider the relaxation process, and $\gamma_{lm,si}$ represents the dephasing rates of $|l,si\rangle \leftrightarrow |m,si\rangle$ transitions. We assume that the atoms are initially populated in one of the two ground-state sublevels, i.e., $\rho_{22,si} = 1$ $(i = 1,2)$.

By solving Eqs. (2a)–(2f) in the steady state, the coherent terms corresponding to the probe transitions can be derived as follows:

$$\rho_{32,s1} = \frac{(\delta_1 - \mathrm{i}\gamma_{12,s1})\,\Omega_{p1}}{(\delta_1 + \Delta_{s1} - \mathrm{i}\gamma_{32,s1})(\delta_1 - \mathrm{i}\gamma_{12,s1}) - \Omega_{s1}^2}, \quad (3a)$$

$$\rho_{31,s2} = -\frac{\Omega_{s2}^2\,(\Delta_{s2} + \mathrm{i}\gamma_{32,s2})^{-1}\,\Omega_{p2}}{(\delta_2 + \Delta_{s2} - \mathrm{i}\gamma_{31,s2})(\delta_2 - \mathrm{i}\gamma_{12,s2}) - \Omega_{s2}^2}. \quad (3b)$$

In this system, the refractive index enhancement of the medium relies on the interaction strength between two Raman transitions, the first of which results in two-photon absorption and the second one contributes two-photon gain to the probe field. Therefore, the total complex susceptibility is equal to the sum of individual contributions from each of the

Λ-type schemes, and the absorption and refractivity can be controlled by changing the two-photon detunings δ_1 and δ_2. According to the polarization of the medium, $P_p = \varepsilon_0 \chi E_p = N_1 \mu_{23,s1} \rho_{32,s1} + N_2 \mu_{13,s2} \rho_{31,s2}$, the susceptibility of the weak probe field can be written as

$$\chi = \chi_1 + \chi_2 = \frac{N_1 \mu_{23,s1}^2 \rho_{32,s1}}{2\varepsilon_0 \hbar \Omega_{p1}} + \frac{N_2 \mu_{13,s2}^2 \rho_{31,s2}}{2\varepsilon_0 \hbar \Omega_{p2}}, \tag{4}$$

where ε_0 is dielectric constant in a vacuum.

Therefore, the susceptibility of the whole system is given by

$$\chi = \frac{1}{2\varepsilon_0 \hbar} \left[\frac{N_1 \mu_{23,s1}^2 (\delta_1 - \mathrm{i}\gamma_{12,s1})}{(\delta_1 + \Delta_{s1} - \mathrm{i}\gamma_{32,s1})(\delta_1 - \mathrm{i}\gamma_{12,s1}) - \Omega_{s1}^2} - \frac{N_2 \mu_{13,s2}^2 \Omega_{s2}^2 (\Delta_{s2} + \mathrm{i}\gamma_{32,s2})^{-1}}{(\delta_2 + \Delta_{s2} - \mathrm{i}\gamma_{31,s2})(\delta_2 - \mathrm{i}\gamma_{12,s2}) - \Omega_{s2}^2} \right]. \tag{5}$$

In order to investigate the coherently induced grating in refractive index enhanced medium, we use two standing-wave fields $\Omega_{s1}(x) = \Omega_{s2}(x) = \Omega_s \sin(\pi x/\Lambda)$ to drive the atoms, with Λ being the spatial period, and assume that the probe field propagates along the z direction through an atomic medium with length L. The propagation of probe field determined by the atomic polarization, which, in the slowly varying envelope approximation and the steady-state regime, can be described by the Maxwell's equation as

$$\frac{\partial E_p}{\partial z} = \mathrm{i}\frac{\pi}{\lambda_p} \chi E_p, \tag{6}$$

where λ_p is the wavelength of the probe field. By solving Eq. (6), the transmission function of the probe field at $z = L$ can be derived as

$$T(x) = \frac{E(L)}{E(0)} = \mathrm{e}^{-\alpha(x)} \mathrm{e}^{\mathrm{i}\phi(x)}. \tag{7}$$

The terms of $\alpha(x) = \pi \mathrm{Im}[\chi] L/\lambda_p$ and $\phi(x) = \pi \mathrm{Re}[\chi] L/\lambda_p$ represent the absorption coefficient and phase shift of the probe field, respectively. According to the Fraunhofer diffraction theory, we obtain the Fraunhofer-diffraction intensity as

$$I(\theta) = |F(\theta)|^2 \frac{\sin^2(M\pi\Lambda \sin\theta/\lambda_p)}{M^2 \sin^2(\pi\Lambda \sin\theta/\lambda_p)}, \tag{8}$$

where $F(\theta) = \int_0^\Lambda T(x) \exp(-\mathrm{i}2\pi x \sin\theta/\lambda_p) \mathrm{d}x$ corresponds to the Fraunhofer diffraction of single spatial period, θ is the diffraction angle with respect to the z direction, and M is the number of spatial periods of the grating. Through Eq. (8) with grating equation $\sin\theta = n\lambda_p/\Lambda$, which determines the n-th order diffraction angle, we can calculate the zeroth-order, first-order and second-order diffraction intensities as follows:

$$I(\theta_0) = \left| \int_0^\Lambda T(x) \mathrm{d}x \right|^2, \tag{9a}$$

$$I(\theta_1) = \left| \int_0^\Lambda T(x) \exp(-\mathrm{i}2\pi x/\Lambda) \mathrm{d}x \right|^2, \tag{9b}$$

$$I(\theta_2) = \left| \int_0^\Lambda T(x) \exp(-\mathrm{i}4\pi x/\Lambda) \mathrm{d}x \right|^2. \tag{9c}$$

In the following, we focus on a real system and consider two Λ schemes in a dual magneto-optical trap of rubidium atomic isotopes with ^{85}Rb (for EIT) and ^{87}Rb (for ARG) using the D_1 line ($\lambda_p = 795$ nm), and assign $|1, s1\rangle = |5^2S_{1/2}, F = 2\rangle$, $|2, s1\rangle = |5^2S_{1/2}, F = 3\rangle$, and $|3, s1\rangle = |5^2P_{1/2}, F = 3\rangle$ for s1-system, and $|1, s2\rangle = |5^2S_{1/2}, F = 1\rangle$, $|2, s2\rangle = |5^2S_{1/2}, F = 2\rangle$, and $|3, s2\rangle = |5^2P_{1/2}, F = 1\rangle$ for s2-system. In the following calculations, the parameters of this atomic system are $N_1 = N_2 = 5.0 \times 10^{12}$ cm^{-3}, $\mu_{23,s1} = \mu_{13,s2} = 2.5377 \times 10^{-29}$ C·m, $\gamma = \gamma_{32,s1} = \gamma_{31,s2} = \gamma_{32,s2} = 5.75$ MHz$/2$, and $\gamma' = \gamma_{12,s1} = \gamma_{12,s2} = 0.05\gamma$. We can manipulate the susceptibility by changing the two-photon detunings δ_1 and δ_2 to obtain diverse phase gratings, and the variations of intensities of driving fields can be used for achieving different phase shifts to enhance the diffraction efficiency.

3. Results and discussion

In order to acquire a high diffraction efficiency for probe beam with the coherently induced grating, we must pay attention to two factors: a large phase shift should be firstly possessed across the probe beam, and the transmission of the probe must be large enough. By using the equations as outlined above, we investigate the formation of phase grating and its diffracting power in this section, and discuss the Fraunhofer diffraction patterns of the probe field in three types of gratings with different phase shifts.

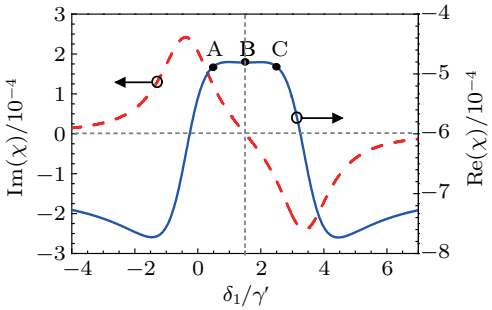


Fig. 2. (color online) Real (solid curve) and imaginary (dash curve) parts of the probe susceptibility versus the two-photon detuning δ_1 under the condition of $\delta_1 - \delta_2 = 3\gamma'$. Parameters are $N_1 = N_2 = 5.0 \times 10^{12}$ cm^{-3}, $\gamma = \gamma_{32,s1} = \gamma_{31,s2} = \gamma_{32,s2} = 5.75/2$ MHz, $\gamma' = \gamma_{12,s1} = \gamma_{12,s2} = 0.05\gamma$, $\Delta_{s1} = -862\gamma$, $\Delta_{s2} = 862\gamma$, and $\Omega_{s1} = \Omega_{s2} = 4\gamma$.

The susceptibility of the medium plays a significant role in the formation of EIG, and we firstly focus on the probe absorption $\mathrm{Im}(\chi)$ and dispersion $\mathrm{Re}(\chi)$. As discussed above, we can efficiently modulate the strength of the two-photon Raman absorption and Raman gain via manipulating the two-photon detunings δ_1 and δ_2 of the laser beams, so that the absorption can be reduced and the probe can even be amplified.

At the same time, the real part of the susceptibility also obtains a large value arising from the constructive contributions of two Raman transitions. In addition, the separation value $\delta_1 - \delta_2$ of two Raman resonances determines the interaction between EIT and ARG systems, and then the refractive index is dependent on the separation of Raman resonances.[42,43] For $\delta_1 - \delta_2 \gg \gamma'$, two Raman transitions are independent of each other and $\mathrm{Re}(\chi)$ drops. But for $\delta_1 - \delta_2 \ll \gamma'$, the effect of two Raman transitions can mutually offset. In such a case, both the absorption and the refraction are cancelled. Therefore, we choose that the separation value of two Raman resonance satisfies $\delta_1 - \delta_2 = 3\gamma'$ here, which is of the order of γ'.[42,43] As shown in Fig. 2, the dispersive part $\mathrm{Re}(\chi)$ and absorptive part $\mathrm{Im}(\chi)$ of the probe susceptibility are plotted separately as a function of two-photon detuning δ_1 for $\delta_1 - \delta_2 = 3\gamma'$, marked with the blue-solid line and red-dashed line, respectively. We take the Rabi frequencies of two driven fields as $\Omega_{s1} = \Omega_{s2} = 4\gamma$. We consider three different conditions for which $\delta_1 = 0.5\gamma'$ (point A), $\delta_1 = 1.5\gamma'$ (point B), and $\delta_1 = 2.5\gamma'$ (point C), respectively. At point B, the absorptive part of susceptibility [$\mathrm{Im}(\chi)$] vanishes due to the balance between two-photon absorption in EIT system and two-photon gain in ARG system while the dispersive part [$\mathrm{Re}(\chi)$] is enhanced due to their constructive contributions. For $\delta_1 < 1.5\gamma'$, the atomic medium is absorptive to probe beam. In this case, the slight deviation from the EIT resonance results in an absorption which is stronger than the gain provided by ARG. However, under the condition of $\delta_1 > 1.5\gamma'$, the Raman gain is dominant and the probe light can be amplified by the atoms. Nevertheless, $\mathrm{Re}(\chi)$ is always enhanced, that is, the atomic system is a refractive index enhanced medium (see points A and C).

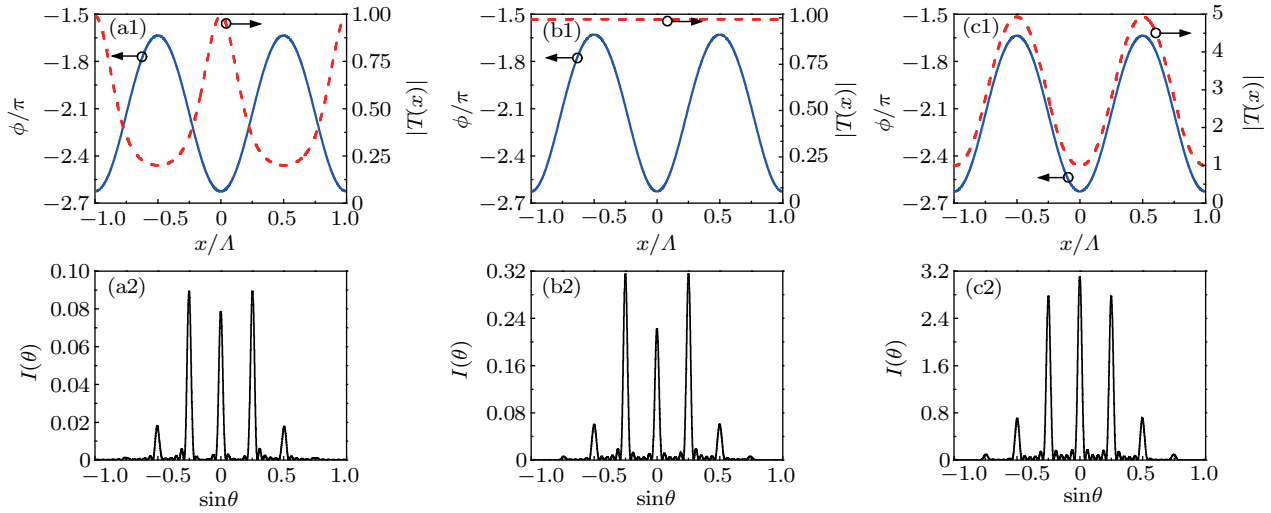


Fig. 3. (color online) Amplitude $|T(x)|$ (red dashed line) and phase $\phi(x)$ (blue solid line) of the transmission function $T(x)$ plotted over two space periods for different two-photon detunings: (a1) $\delta_1 = 0.5\gamma'$, $\delta_2 = -2.5\gamma'$; (b1) $\delta_1 = 1.5\gamma'$, $\delta_2 = -1.5\gamma'$; (c1) $\delta_1 = 2.5\gamma'$, $\delta_2 = -0.5\gamma'$. ((a2), (b2), and (c2)): Plots of diffraction pattern $I(\theta)$ versus $\sin\theta$ corresponding to the (a1), (b1), and (c1) cases. Parameters are Ω_s=4.5γ, $L = 3$ mm, $M = 6$, and $\Lambda = 4\lambda_p$. Other parameters are the same as those in Fig. 2.

The strength of the two-photon absorption in EIT system and the two-photon gain in ARG system are dependent on the amplitudes of the coupling fields [see Eq. (5)]. Then coupling fields with standing-wave pattern can result in a spatially modulated grating for the probe fields. As shown in Fig. 3, the properties of grating are different for the probe field when two-photon detunings of the two Raman transitions δ_1 and δ_2 take different values. With the parameters fixed, a large phase modulation is observed, reaching a peak phase-shift value of π at $x = \pm 0.5\Lambda$ for $\Omega_s = 4.5\gamma$ [see the solid lines in Figs. 3(a1)–(a3)]. However, the amplitude modulations vary with different two-photon detunings [see the dashed lines in Figs. 3(a1)–(a3)]. Figure 3(a1) shows the transmission function for the two-photon detunings of $\delta_1 = 0.5\gamma'$ and $\delta_2 = -2.5\gamma'$. There is a certain amplitude modulation of transmission function, which oscillates around an average transmissivity of 46.8% along the x direction in a period of Λ. Therefore, the probe field has a significant energy loss inside the atomic medium due to the absorption effect in the EIT system with non-zero two-photon detuning. This is a limit to the diffracting power of the atomic grating. The resulting first-order diffraction efficiency of grating reaches only to 8.9% as shown in Fig. 3(a2). Thus, this grating is a mixture of an absorption grating and a phase grating. Figure 3(b1) shows the transmission function for $\delta_1 = 1.5\gamma'$ and $\delta_2 = -1.5\gamma'$. We can obtain a phase modulation of the order of π for the probe beam with extremely low energy loss in the atomic medium, which is due to a good balance between the two-photon absorption in EIT system and the two-photon Raman gain in ARG system. As a result, a pure phase grating with nearly 100% transmissivity is developed in the medium and the diffraction efficiency of probe beam is improved. The energy diffracted into the first-order direction

can reach to 31.5%, which means that this EIG is very close to an ideal sinusoidal phase grating (about 34%) as shown in Fig. 3(b2). In the same way, we plot the transmission function with the detunings being δ_1=2.5γ' and $\delta_2 = -0.5\gamma'$ in Fig. 3(c1). It shows that the amplitude modulation of transmitted probe light is periodically modulated in space with an average transmissivity large than 100% which corresponds to an amplification of the probe beam. At the same time, the resulting phase modulation within a period is still π. Here, the probe gain is attributed to the effect of ARG. The far-field diffraction pattern of this grating is depicted in Fig. 3(c2). It is clear that the first-order diffraction efficiency can exceed 100%. Therefore, a kind of gain-phase grating is obtained. From Figs. 3(a2), 3(b2), and 3(c2), we can observe that a small amount of energy is also shifted into the second diffraction orders which are located at $\sin\theta = \pm 0.5$, and the diffraction efficiency is enhanced with the increase of total transmittance.

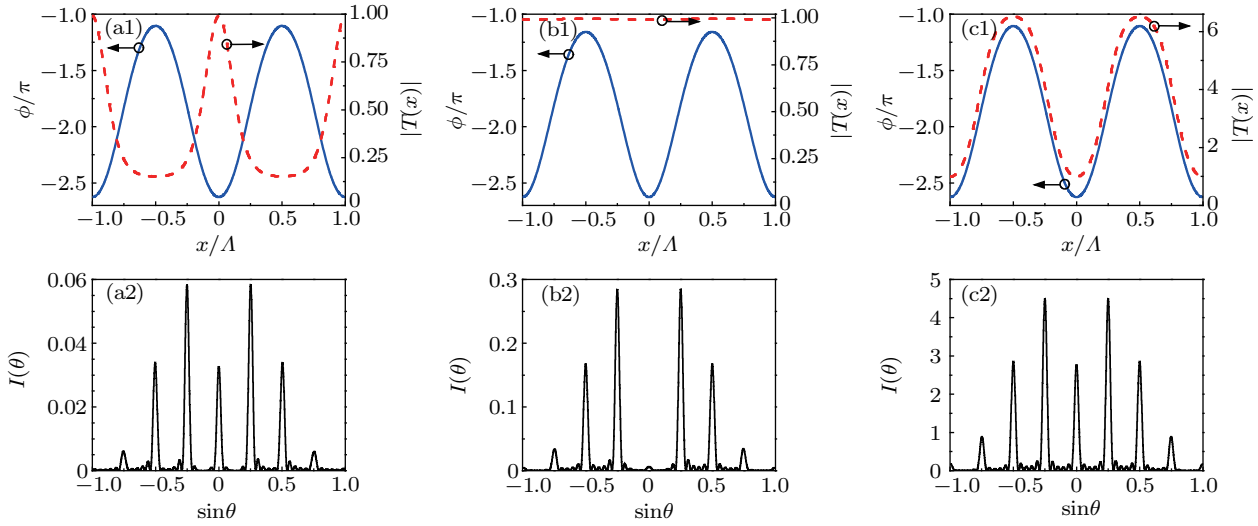


Fig. 4. (color online) Amplitude $|T(x)|$ (red dashed line) and phase $\phi(x)$ (blue solid line) of the transmission function $T(x)$ plotted over two space periods for different two-photon detunings: (a1) $\delta_1 = 0.5\gamma'$, $\delta_2 = -1.5\gamma'$; (b1) $\delta_1 = 1.5\gamma'$, $\delta_2 = -1.5\gamma'$; (c1) $\delta_1 = 2.5\gamma'$, $\delta_2 = -0.5\gamma'$ when $\Omega_s = 5.8\gamma$. [(a2), (b2), and (c2)] Diffraction patterns $I(\theta)$ as a function of $\sin\theta$ for the (a1), (b1), and (c1) cases. Other parameters are the same as those in Fig. 3.

The diffraction efficiency depends on the two-photon detunings δ_1 and δ_2 and the intensity of driving standing-wave field Ω_s. Figure 4 displays the changes of transmission function and diffraction pattern for $\Omega_s = 5.8\gamma$. Other parameters are the same as those in Fig. 3. It is obvious that we can obtain a phase modulation of the order of 1.5π at $x = \pm 0.5\Lambda$ [see the solid lines of Figs. 4(a1), 4(b1), and 4(c1)]. However, the amplitude modulation $|T(x)|$ varies with two-photon detuning. For the cases of $\delta_1 = 0.5\gamma'$ and $\delta_2 = -2.5\gamma'$, the amplitude modulation is plotted in Fig. 4(a1) with the dashed line. Its average transmissivity is about 38.2%. Hence, the medium absorbs more energy from the probe beam than that of the case in Fig. 3(a1). It is due to the increased two-photon absorption in EIT system. The diffraction intensity corresponding to this absorption-phase grating is plotted in Fig. 4(a2). Comparing Fig. 4(a2) with Fig. 3(a2), we can see that more probe energy is deflected into the second order diffraction peaks. This is due to the improvement of phase modulation. When the detunings are $\delta_1 = 1.5\gamma'$ and $\delta_2 = -1.5\gamma'$, we can see that there is no amplitude modulation as shown in Fig. 4(b1) with the dashed line. Consequently, a pure-phase grating is built up in the medium. Almost all the energy in the probe beam is diffracted into the first-order and second-order directions with nearly no light left in zeroth-order [see Fig. 4(b2)]. The diffraction efficiency is enhanced by comparing with Fig. 3(a2). In Figs. 4(c1) and 4(c2), we also plot, respectively, the transmission function $|T(x)|$ and diffraction pattern $I(\theta)$ for detunings $\delta_1 = 2.5\gamma'$ and $\delta_2 = -0.5\gamma'$. There is a periodical gain modulation for probe field, which leads to a structure of gain-phase grating, and therefore the diffraction efficiencies of high-order directions are significantly enhanced. As shown in Fig. 4(c2), the corresponding values of each high-order diffraction intensity increase to $I(\theta_1) = 450\%$ at $\sin\theta_1 = \pm 0.25$ and $I(\theta_2) = 306\%$ at $\sin\theta_2 = \pm 0.5$.

Additionally, comparing the corresponding graphs in Figs. 3 and 4, it is found that the depth of phase modulation and the diffraction efficiency are dependent on the Rabi frequency of coupling field. The phase modulation makes the probe light mainly disperse into the high-order directions. Meanwhile, the amplification of probe beam from the Raman gain can enhance the diffraction efficiencies of all orders.

In order to further clearly clarify the effect of coupling field intensity on diffraction efficiency, we display the variations of the different order diffraction intensities $I(\theta_0)$, $I(\theta_1)$, and $I(\theta_2)$ with coupling field intensity Ω_s for different values of δ_1 and δ_2 in Fig. 5. It is found that the $I(\theta_0)$ decreases as Ω_s

increases as shown with the solid lines in Figs. 5(a) and 5(b) for the absorption-phase gratings and phase gratings. But for the case of gain-phase grating ($\delta_1 = 2.5\gamma'$ and $\delta_2 = -0.5\gamma'$), the zeroth-order diffraction intensity $I(\theta_0)$ firstly presents two gain peak at a certain Ω_s, beyond which it declines for large Ω_s as shown with solid line in Fig. 5(c). Then the high-order diffraction intensities $I(\theta_1)$ and $I(\theta_2)$ can successively increase as Ω_s further increases, and they can take their maximum values under an appropriate Ω_s with the dashed and dashed-dotted lines shown in Figs. 5(a)–5(c), respectively. Moreover, the maximum values of $I(\theta_1)$ and $I(\theta_2)$ are not equivalent to each other for different conditions of δ_1 and δ_2. As a result, the probe light can be diffracted into first-order and higher order directions and the diffracting power of gratings can be also enhanced at the same time by modulating the intensity Ω_s of coupling fields. It is because the phase modulation is enlarged with the increase of Ω_s, which makes more probe energy deflect into the high-order directions. Therefore, these gratings can be applied to the all-optical multi-channel beam splitting and switching for optical networking and communication.

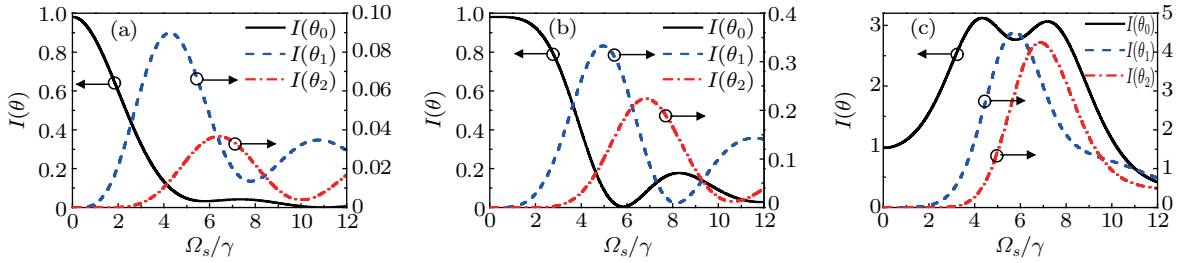


Fig. 5. (color online) Diffraction intensities of zeroth-order $I(\theta_0)$ (black solid line), first-order $I(\theta_1)$ (blue dashed line), and second-order $I(\theta_2)$ (red dashed-dotted line) versus coupling field intensity Ω_s for (a) $\delta_1 = 0.5\gamma'$, $\delta_2 = -1.5\gamma'$; (b) $\delta_1 = 1.5\gamma'$, $\delta_2 = -1.5\gamma'$; (c) $\delta_1 = 2.5\gamma'$, $\delta_2 = -0.5\gamma'$. Other parameters are the same as those in Fig. 3.

4. Conclusions and perspectives

In this paper, by using two standing-wave fields, we propose a scheme for coherently induced grating in a mixture of two three-level atomic species with EIT and ARG systems. Three types of phase gratings are investigated in a real atomic system with ^{85}Rb and ^{87}Rb. By using the interaction between the two two-photon resonances, we obtain an enhanced refractive index in the medium. As a result of intensity dependent standing-wave fields, amplitude and phase are modulated periodically in space, and then a sinusoidal grating will be formed. It is shown that different diffraction patterns can be obtained by varying the two-photon detunings δ_1 and δ_2. The two-photon absorption in EIT system and Raman gain in ARG system contribute to the amplitude modulation, which affects the diffraction efficiency of the induced gratings. Meanwhile, we can achieve different phase-shift values by changing the intensities of two standing-wave fields. A larger phase modulation depth can help to deflect the probe energy into the higher order diffraction directions. The intensities of two standing-wave fields have an important influence on the diffraction efficiency of gratings, thereby the diffraction intensities $I(\theta_0)$, $I(\theta_1)$, and $I(\theta_2)$ of different orders can take their maximum values at appropriate Ω_s. Therefore, it is necessary to choose appropriate parameters to achieve the required diffraction and splitting of probe beam. Thus, the proposed gratings may be employed as all-optical splitter and switching in optical networking and communication. Moreover, in addition to cold atoms, EIG can be formed in thermal atoms.[19,46] Hence, our scheme can also be performed with hot rubidium atoms.[42]

References

[1] Harris S E 1997 *Phys. Today* **50** 36
[2] Fleischhauer M, Imamoglu A and Marangos J P 2005 *Rev. Mod. Phys.* **77** 633
[3] Dalton B J, McDuff R and Knight P L 1985 *Opt. Acta* **32** 61
[4] Gray H R, Whitley R M and Stroud C R 1978 *Opt. Lett.* **3** 218
[5] ZhuY F 1992 *Phys. Rev. A* **45** R6149
[6] Fry E S, Li X and Nikonov D 1993 *Phys. Rev. Lett.* **70** 3235
[7] Scully M O 1991 *Phys. Rev. Lett.* **67** 1855
[8] Proite N A, Unks B E, Green J T and Yavuz D D 2008 *Phys. Rev. Lett.* **101** 147401
[9] Hau L V, Harris S E, Dutton Z and Behroozi C H 1999 *Nature* **397** 594
[10] Kash M M, Sautenkov V A, Zibrov A S, Hollberg L, Welch G R, Lukin M D, Rostovtsev Y, Fry E S and Scully M O 1999 *Phys. Rev. Lett.* **82** 5229
[11] Liu C, Dutton Z, Behroozi C H, and Hau L V 2001 *Nature* **409** 490
[12] Longdell J J, Fraval E, Sellars M J and Manson N B 2005 *Phys. Rev. Lett.* **95** 063601
[13] Wang H, Goorskey D and Xiao M 2001 *Phys. Rev. Lett.* **87** 073601
[14] Kang H and Zhu Y F 2003 *Phys. Rev. Lett.* **91** 093601
[15] Wu Y and Deng L 2004 *Phys. Rev. Lett.* **93** 143904
[16] Huang G X, Deng L and Payne M G 2005 *Phys. Rev. E* **72** 016617
[17] Ling H Y, Li Y Q and Xiao M 1998 *Phys. Rev. A* **57** 1338
[18] Mitsunaga M and Imoto N 1999 *Phys. Rev. A* **59** 4773
[19] Sheng J T, Wang J, Miri M A, Christodoulides D N and Xiao M 2015 *Opt. Express* **23** 19777
[20] Zhai P W, Su X M and Gao J Y 2001 *Phys. Lett. A* **289** 27
[21] Brown A W and Xiao M 2005 *Opt. Lett.* **30** 699
[22] Zhao L, Duan W and Yelin S F 2010 *Phys. Rev. A* **82** 013809
[23] Wen J M, Du S W, Chen H Y and Xiao M 2011 *Appl. Phys. Lett.* **98** 081108
[24] Chen H X, Zhang X, Zhu D Y, Yang C, Jiang T, Zheng H B and Zhang Y P 2014 *Phys. Rev. A* **90** 043846
[25] Zha X W, Yuan C Z and Zhang Y P 2013 *Laser Phys. Lett.* **10** 045201
[26] Zhang Y Q, Wu Z K, Belić M R, Zheng H B, Wang Z G, Xiao M and Zhang Y P 2015 *Laser Photon. Rev.* **9** 331

[27] de Araujo L E E 2010 *Opt. Lett.* **35** 977
[28] Wan R G, Kou J, Jiang L, Jiang Y and Gao J Y 2011 *Phys. Rev. A* **83** 033824
[29] Zhou F X, Qi Y H, Sun H, Chen D J, Yang J, Niu Y P and Gong S Q 2013 *Opt. Express* **21** 12249
[30] Cheng G L, Zhong W X, and Chen A X 2015 *Opt. Express* **23** 9870
[31] Liu J B, Liu N, Shan C J, Liu T K, Li H, Zheng A S and Xie X T 2016 *Phys. Lett. A* **380** 2458
[32] Xiao Z H, Shin S G and Kim K 2010 *J. Phys. B: At. Mol. Opt. Phys.* **43** 161004
[33] Dong Y B and Guo Y H 2014 *Chin. Phys. B* **23** 074204
[34] Liu Y, Wang P and Peng S Y 2013 *Chin. Phys. B* **22** 104203
[35] Yu S, Liao P, Yang Z Y and Gu W Y 2013 *Acta Phys. Sin.* **62** 224205 (in Chinese)
[36] Kuang S Q, Jin C S and Li C 2011 *Phys. Rev. A* **84** 033831
[37] Wang L, Zhou F X, Hu P D, Niu Y P and Gong S Q 2014 *J. Phys. B: At. Mol. Opt. Phys.* **47** 225501
[38] Wu J C and Ai B Q 2015 *J. Phys. B: At. Mol. Opt. Phys.* **48** 115504
[39] Wang L, Zhou F X, Guo H J, Niu Y P and Gong S Q 2016 *Chin. Phys. B* **25** 114205
[40] Chen Y Y, Liu Z Z and Wan R G 2016 *Europhys. Lett.* **116** 64006
[41] Chen Y Y, Liu Z Z and Wan R G 2017 *Phys. Lett. A* **381** 1362
[42] Proite N A, Unks B E, Green J T and Yavuz D D 2008 *Phys. Rev. Lett.* **101** 147401
[43] O'Brien C, Anisimov P M, Rostovtsev Y and Kocharovskaya O 2011 *Phys. Rev. A* **84** 063835
[44] Hang C, Huang G X and Konotop V K 2013 *Phys. Rev. Lett.* **110** 083604
[45] Pei L Y, Lu X G, Bai J H, Miao X X, Wang R Q, Wu L A, Ren S W, Jiao Z Y, Zhu H F, Fu P M and Zuo Z C 2013 *Phys. Rev. A.* **87** 063822
[46] Dong Y B, Li J Y and Zhou Z Y 2017 *Chin. Phys. B* **26** 014202